ONCOIMMUNOLOGY
2018, VOL. 7, NO. 4, e1397248 (12 pages)
https://doi.org/10.1080/2162402X.2017.1397248

Taylor & Francis
Taylor & Francis Group

ORIGINAL RESEARCH



# Anti-CD47 treatment enhances anti-tumor T-cell immunity and improves immunosuppressive environment in head and neck squamous cell carcinoma

Lei Wu[a], Guang-Tao Yu[a], Wei-Wei Deng[a], Liang Mao[a], Lei-Lei Yang[a], Si-Rui Ma[a,b], Lin-Lin Bu[a,b], Ashok B. Kulkarni[c], Wen-Feng Zhang[a,b], Lu Zhang[a], and Zhi-Jun Sun[a,b,c]

[a]The State Key Laboratory Breeding Base of Basic Science of Stomatology & Key Laboratory of Oral Biomedicine, Ministry of Education, Wuhan, Hubei, China; [b]Department of Oral Maxillofacial-Head Neck Oncology, School and Hospital of Stomatology, Wuhan University, Wuhan, Hubei, China; [c]Functional Genomics Section, Laboratory of Cell and Developmental Biology, National Institute of Dental and Craniofacial Research, National Institutes of Health, Bethesda, MD USA

**ABSTRACT**

Head and neck squamous cell carcinoma (HNSCC) is considered as an immunosuppressive disease, with impaired tumor-infiltrating T lymphocytes and increased suppressive immune cells. The efficacy of CD47 antibodies in immune checkpoint therapy is not clearly understood in HNSCC. In this study, human tissue microarrays and immunocompetent transgenic mouse models were used to explore the expression of CD47 and the use of CD47 antibodies in HNSCC. We identified overexpression of CD47 in HNSCC as compared with the control normal human tissue and also in HNSCC mouse models. The expression of CD47 also correlated with clinicopathological parameters as well as outcome. Furthermore, inhibition of CD47 delayed tumor growth and improved tumor microenvironment by stimulating effector T cells and decreasing suppressive immune cells and regulating the function of $CD11b^{+}$ $Ly6G^{+}$ MDSC. Our data suggest that CD47 blockade may be a potential immunotherapeutic target in human HNSCC.

**ARTICLE HISTORY**
Received 5 June 2017
Revised 6 October 2017
Accepted 21 October 2017

**KEYWORDS**
CD47; HNSCC; immunotherapy; tissue microarrays; transgenic mouse model

## Introduction

The hallmarks of cancer including sustaining proliferative signaling, evasion of growth suppressors, and resistance to apoptosis, replicative immortality, and escaping the immune destruction lead to initiation and progression of cancer.[1] Cancer cells have various strategies to avoid recognition and destruction by the immune system, thereby evading immune surveillance.[1] Many immune cells play a key role in evading immune surveillance in the tumor microenvironment of head and neck squamous cell carcinoma (HNSCC) including myeloid-derived suppressor cells (MDSCs), regulatory T cells (Tregs) and tumor-associated macrophages (TAMs).[2] MDSCs represent a diverse immunosuppressive cell population in various cancer types, inhibiting activated T cells, impairing natural killer (NK) cells, and facilitating stem cell-like cancer cells.[3–6] MDSCs identified by expression of CD11b and Gr-1 (Ly6C+/Ly6G+) in mice, and the subpopulations of MDSCs have also been defined as polymorph nuclear ($CD11b^{+}Ly6G^{+}Ly6C^{lo}$) (PMN) and monocytic ($CD11b^{+}Ly6G^{-}Ly6C^{hi}$) (M)-MDSCs.[7] The $CD4^{+}CD25^{+}Foxp3^{+}$ regulatory T cells (Tregs) promote tumor progression by regulating the immune system with the inhibition of actions of activated T cells in peripheral lymphoid tissues.[8]

CD47, a "don't eat me" signal for phagocytic cells, is expressed on the surface of multiple human tumor types including ovarian carcinomas, renal cell carcinoma (RCC), human hepatocellular carcinoma (HCC), acute myeloid leukemia (AML) and other human solid tumor.[9–12] CD47 expressed on tumor cells evade immune surveillance through binding to signal regulatory protein-$\alpha$ (SIRP$\alpha$), a protein expressed on macrophages and dendritic cells, thereby resulting in the inhibition of phagocytosis.[13] CD47 also binds to thrombospondin-1 (TSP1), which is a ligand in T cells of CD47,[14] to inhibit T-cell activation in the immune system.[15,16] Recent reports indicated that CD47 is involved in the process of adaptive immunity response by impairing T cell immune response.[17,18] Blockade of CD47 led to an efficient and rapid elimination of multiple tumor cell types and achieved a good effect in the malignant tumor.[19,20]

Immune checkpoint molecules such as programmed cell death protein 1 (PD1) are the major mechanism of immune resistance, particularly dampening T cell activation to avoid tumor cell elimination.[21] Immune checkpoint blockade, enhancing T cell antitumor activity and revitalizing suppressed immune environment, have produced encouraging results in the treatment of multiple cancers including head neck cancer.[8] Recent studies reported that antibody blockade of CD47 enhances NK cell-mediated killing of HNSCC cells *in vitro* and CD47 suppression increased tumor delay *in vivo* using the SCC VII HNSCC model in immune competent mice.[22, 23] Using the same mouse model, David *et al.* reported that anti-CD47 treatment induced tumor delay depends on T cell–mediated antitumor immunity.[17] In order to further explore the efficiency of the anti-CD47 treatment as another immune checkpoint therapy, we utilized our HNSCC mouse model for *in vivo* experiments.

**CONTACT** Zhi-Jun Sun sunzj@whu.edu.cn School and Hospital of Stomatology, Wuhan University, Wuhan, 430079, China.
Lu Zhang, School and Hospital of Stomatology, Wuhan University, Wuhan, 430079, China. e-mail: luzhang2012@whu.edu.cn.

The present study was designed to investigate the precise effect of CD47 inhibition in the modulation of tumor infiltrating T cells, MDSCs, Tregs and immune checkpoint molecules in HNSCC.

## Results

### *Overexpression of CD47 in HNSCC tissue and dysplasia is associated with clinical outcome of primary HNSCC*

Many studies suggested that CD47 was overexpressed in multiple types of cancers.[9,10,12,24] This prompted us to gain insight into the expression of CD47 in HNSCC and normal mucosa. We identified mRNA and DNA expression of CD47 in human HNSCC by Oncomine database.[25] *CD47* mRNA or DNA copy number were significantly increased in 13 out of 17 HNSCC datasets (Fig. S1). Moreover, analysis of Cromer and TCGA dataset revealed significant increase in the mRNA level and DNA copy number of *CD47* in HNSCC as compared with their control counterpart (Fig. S1). Furthermore, immunohistochemical staining of specimen from 48 cases of oral mucosa, 43 cases of dysplasia (Dys) and 165 cases of primary HNSCC showed higher CD47 expression in human HNSCC tissue as

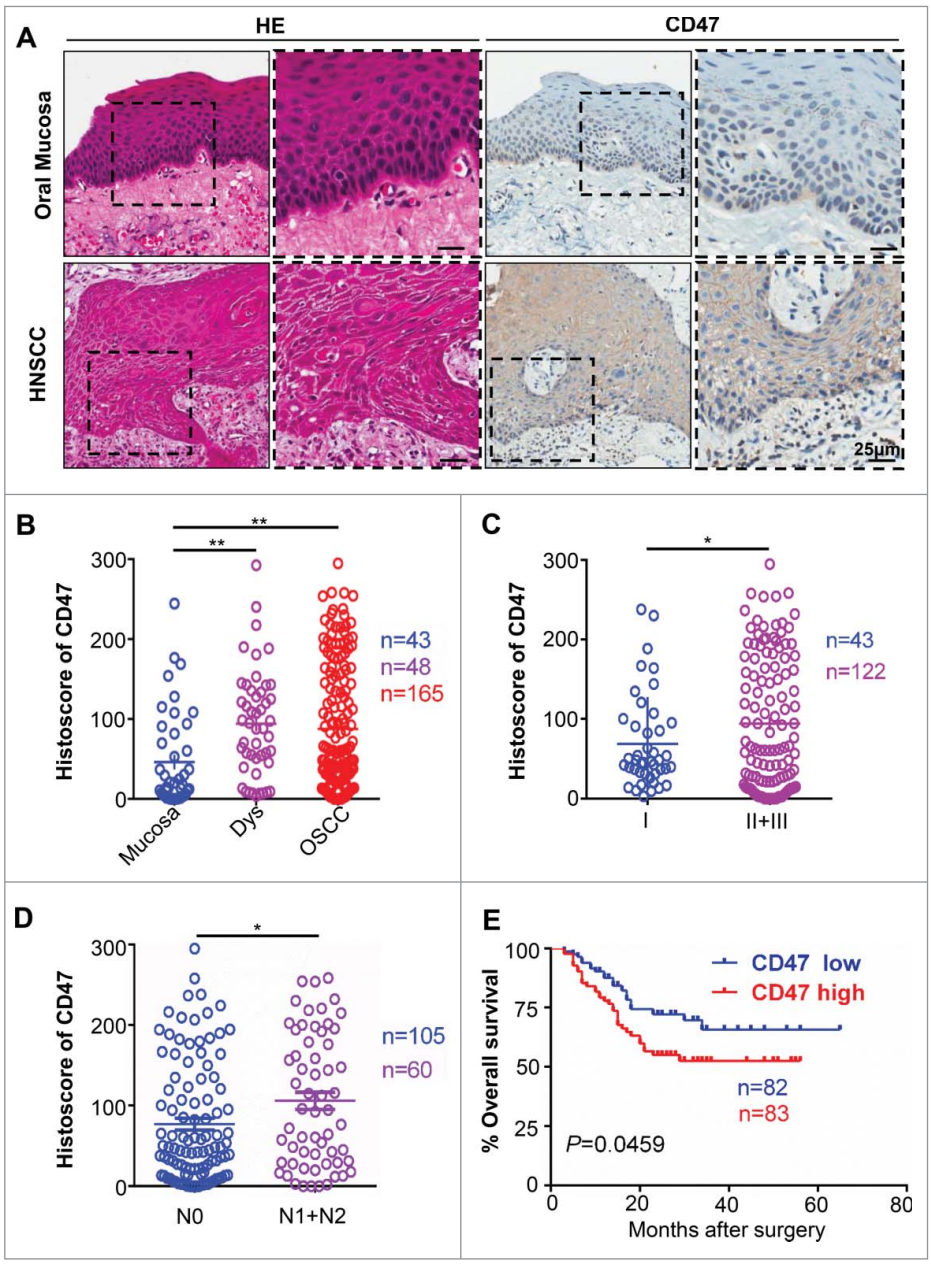


**Figure 1.** Overexpression of CD47 in human HNSCC confers poor prognosis of HNSCC patients. Representative hematoxylin-eosin, immunohistochemical staining (A) and quantification (B) of CD47 in human head neck squamous cell carcinoma (HNSCC, $n = 165$) as compared with dysplasia (Dys, $n = 48$) and oral mucosa ($n = 43$). Each dot is presented as an independent core. CD47 staining was significantly alternated in different pathological grades (C, Grade II+III vs Grade I, $P<0.05$), the primary tumor with positive or negative lymph node metastasis status (D, N1+N2 vs N0, $P<0.05$). (E) Kaplan–Meier survival analysis indicated that high CD47 expression confers poor overall survival in the patient with HNSCC ($P$-value = 0.0495) with the median of CD47 protein expression histoscore (the histoscore = 58.37) as a cut-off.

compared with normal oral mucosa. Interestingly, positive immunostaining of CD47 was mainly localized in cancer cells, especially in the invasive layer of cancer cells (Fig. 1A). Quantification of CD47 expression also showed that CD47 was significantly increased in human HNSCC tissue and dysplasia as compared with in oral mucosa (Fig. 1B). Further detailed analysis of HNSCC tissue revealed that CD47 staining was significantly increased in advanced pathology grade HNSCC (II+III vs. I, $P<0.05$, Fig. 1C) and primary HNSCC with lymph node metastasis (N1+N2 vs. N0, $P < 0.05$, Fig. 1D). Most importantly, in 165 primary HNSCC with follow-up data, Kaplan–Meier survival analysis indicated that CD47 high expression confers poor overall survival in the patient with HNSCC (n = 165, $P$-value = 0.0459, Fig. 1E) with the median of CD47 protein expression histoscore (the histoscore = 58.37) as a cut-off value.

### *Overexpression of CD47 in human HNSCC is associated with PD-1/PD-L1, Foxp3 and myeloid-derived suppressor cell markers*

Cumulative studies demonstrated that overexpression of CD47 may correlate with immunosuppressive status,[26] including elevated expression inhibitory marker PD-1 and PD-L1, accumulation of Treg and MDSCs.[27] This finding prompted us to determine the correlation between the CD47 and suppressive cells. We analyzed the PD-1, PD-L1, Foxp3 and MDSC markers (CD11b and CD33) by immunohistochemical staining in human HNSCC as shown in Fig. 2A. The expression of CD47 was positively correlated with PD-1 ($P<0.001$) and PD-L1 ($P<0.01$, Fig. 2B). Similarly, the expression of Treg marker Foxp3 ($P<0.001$) and MDSC markers CD11b ($P<0.01$) and CD33 ($P<0.01$) was positively correlated with the CD47 (Fig. 2C). Hierarchical clustering indicated that CD47

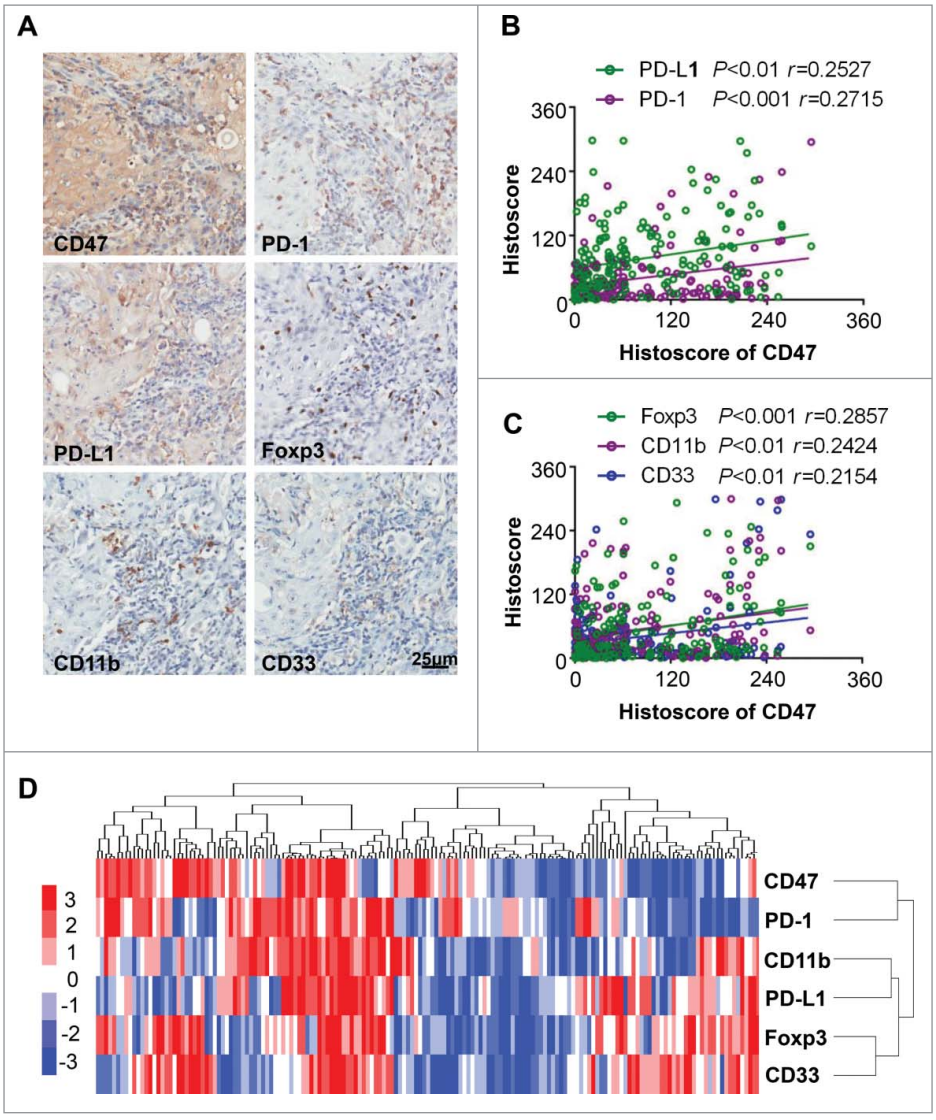


**Figure 2.** Overexpression of CD47 in human HNSCC is associated with inhibitory checkpoints and suppressive immune cell. (A) Representative immunohistochemical staining of CD47, PD-1, PD-L1, Foxp3, CD11b and CD33 in human HNSCC specimens. Scale bar, 25 $\mu$m. (B) The expression of CD47 was positively correlated with PD-1 ($P<0.001$, $r = 0.2715$) and PD-L1 ($P <0.01$, $r = 0.2527$). (C) The expression of CD47 were positively correlated with Foxp3 ($P<0.001$, $r = 0.2857$), CD11b ($P<0.01$, $r = 0.2424$) and CD33 ($P<0.01$, $r = 0.2154$) in human HNSCC. (D) Hierarchical clustering indicated a close relation of CD47 with PD-1 in primary HNSCC. (statistic including 165 primary HNSCC).

expression may mostly correlate with PD-1 expression in the human HNSCC sample (Fig. 2D). Together, these results suggest that the activation of CD47 is correlated with PD-1/PD-L1 expression, Tregs, and MDSCs in human HNSCC.

### *Anti-CD47 treatment delays tumor growth in Tgfbr1/Pten 2 cKO HNSCC mouse model*

Loss of *PTEN* has been described as a frequent molecular event in HNSCC.[28] Conditional deletion of the tumor suppressor *Tgfbr1* in epithelial cells, which abrogates TGF-$\beta$ signaling, leads to accumulation of TGF-$\beta$1 ligands in stromal cells.[29,30] A combined deletion of important tumor suppressors *Pten* and *Tgfbr1* (2 cKO) leads to a fast and full penetration of HNSCC tumorigenesis in these mice.[31] Pathologically, the HNSCC mice were similar to human HNSCC with abundant infiltration of inflammatory cells.[31] Considering the negative role and rather high expression of CD47 in human HNSCC, we subsequently examined the expression of CD47 in this mice model. As shown in Fig. 3A, CD47 was highly expressed in mouse HNSCC compared with wild-type mouse. The results of Western blot and immunofluorescence were consistent with

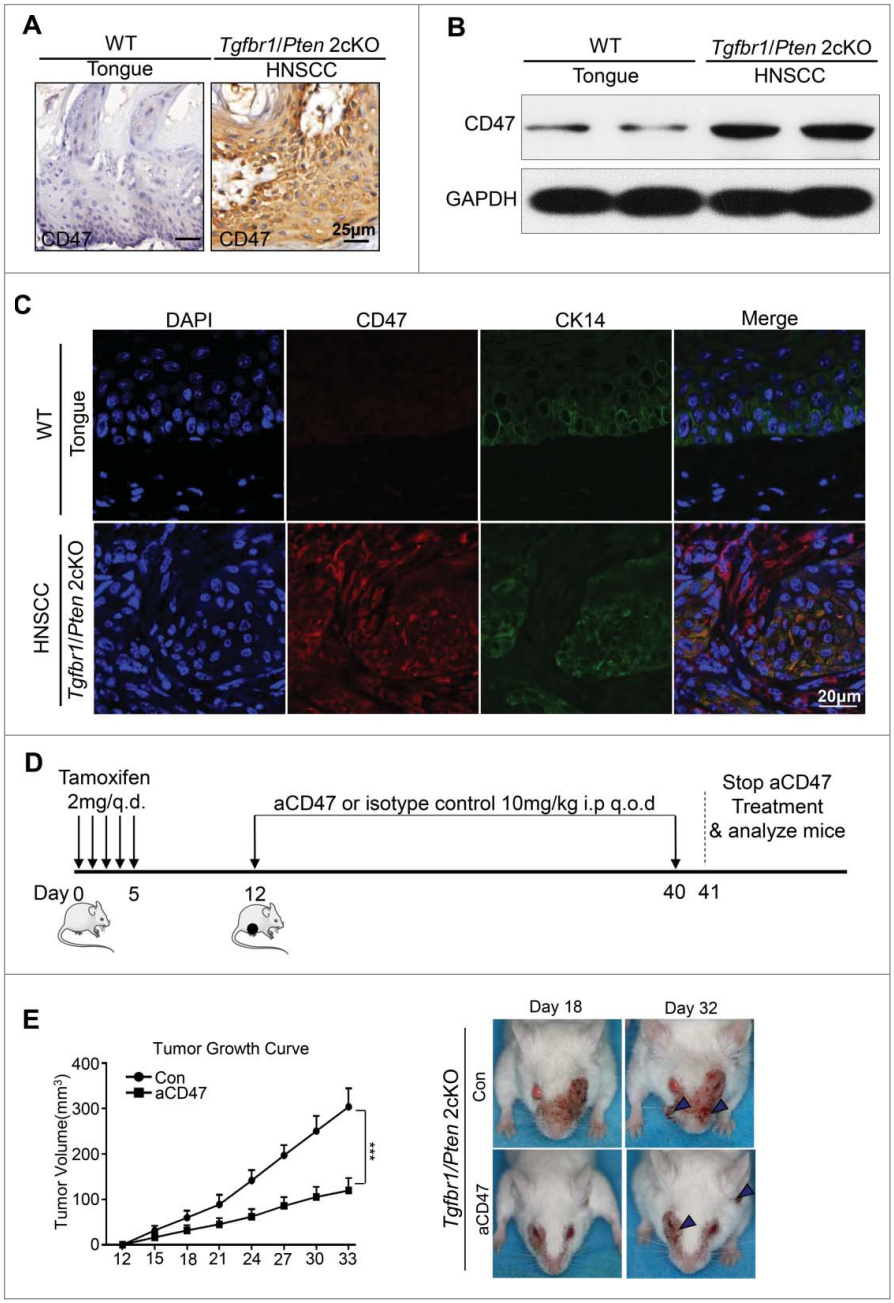


**Figure 3.** Anti-CD47 treatment by monoclonal antibody delays tumorigenesis in immunocompetent transgenic HNSCC mouse models. Representative immunohistochemical staining (A), western blot with GAPDH as a loading control of CD47 (B) and immunofluorescence staining for CD47 (red immunofluorescene), CK14 (green) and nucleus (blue) (C) in *Tgfbr1/Pten* 2cKO mice HNSCC compared with wild-type tongue. (D) *Tgfbr1/Pten* 2cKO mice bearing carcinoma by tamoxifen were treated with the CD47 antibody ($\alpha$CD47) intraperitoneally (i.p) every other day for 28 days or isotype control treated ($n = 5$ mice respectively). (E) Tumor burden and representative photos of mice with head and neck tumor (right panel) after treatment with $\alpha$CD47 or isotype IgG in day 18 and day 32 after tamoxifen gavage. Data presented as mean $\pm$ SEM.

that of immunohistochemical staining (Fig. 3B and C). Based on this finding, specific mouse CD47 monoclonal antibody was used to explore the role of CD47 in this mouse model. To test the effect of CD47 on the progression of HNSCC *in vivo*, a chemopreventive investigation on the *Tgfbr1/Pten* 2 cKO mouse model was performed. The mice received the intraperitoneal injection of CD47 blocking antibody (MIAP301, known to functionally blockade CD47-SIRP$\alpha$ interactions,[18] rat IgG2a$\kappa$, 10 mg/kg per mouse; n = 5 mice respectively) or isotype control rat IgG2a$\kappa$ (2A3, 10 mg/kg per mouse; n = 5 mice respectively) every other day (Fig. 3D). Tumor growth was assessed every third day by direct measurements of tumor size. We observed that the tumor burden of head and neck sufficiently reduced by systemic anti-CD47 treatment (Fig. 3E). Meanwhile, the results of body weight changes in two groups indicated that treatment with an anti-mouse-CD47 mAb did not cause significant weight changes between CD47 blockade and control group ($P>0.05$, Fig. S2A). There were no significant differences between the anti-CD47 treatment group and control group in major organs using H&E staining (Fig. S2B), indicating that we did not identify readily detectable cytotoxicity in our mouse model upon anti-CD47 treatment. Together, these results show that inhibition of CD47 suppresses HNSCC progression. In addition, anti-CD47 treatment effectively rescued immunosuppressive status as indicated by the decrease of spleen index and size of lymph node (Fig. S2 C and D).

### Anti-CD47 treatment reduced PD-1 expression and increased IFN-$\gamma$ secretion in the effector T cells of HNSCC mouse model

Based on the significant effect on peripheral immune organs with anti-CD47 treatment, we hypothesized that the tumor-bearing *Tgfbr1/Pten* 2cKO mouse was in an immunosuppressive state in the tumor progression. Considering that elevated and sustained expression of PD-1 in T cells is a hallmark of T cell exhaustion,[32] we first wanted to answer whether anti-CD47 treatment could decrease PD-1 expression on T cell population in this mouse model. The single cell suspension from the spleen, LN, blood, and tumor were stained by antibody for PD-1, CD4, and CD8. Indeed, anti-CD47 treatment remarkably decreased the rate of PD-1$^+$CD4$^+$ and PD-1$^+$CD8$^+$ T cells in spleen, peripheral blood and tumor microenvironment (Fig. S3A, Fig. 4A and B). Moreover, flow cytometry indicated that INF-$\gamma$ in CD8+ tumor infiltrating T cell in anti-CD47 treated mice was increased (Fig. 4C). The results were also confirmed by immunohistochemistry of PD-1 and INF-$\gamma$ (Fig. 4D). Together, these observations suggest that CD47 antibody treatment can effectively reinvigorate effector T cells in HNSCC mouse model.

### Anti-CD47 treatment reduces CD4+ Foxp3+ Tregs and MDSCs of HNSCC mouse model

Our previous findings indicated that the immunosuppressive cells are involved in the tumor-bearing *Tgfbr1/Pten* 2cKO mouse with increased Tregs.[33] Therefore, in order to explore the potential effect of the anti-CD47 treatment on these immunosuppressive cells, the population of CD4$^+$ CD25$^+$ Foxp3$^+$ Tregs in isotype control mice and anti-CD47 treated mice were analyzed by flow cytometry. Compared with vehicle group, anti-CD47 treatment significantly reduced the population of CD4$^+$ CD25$^+$ Foxp3$^+$ Tregs in the spleen, lymph nodes, peripheral blood and tumor (Fig. S3B, Fig. 5A and B). The result was confirmed by immunohistochemical staining of Foxp3 in CD47 treated mice as compared with isotype control counterpart (Fig. 5C). These results demonstrated that anti-CD47 treatment effectively reduced the population of Tregs in 2cKO tumor-bearing mice. MDSCs were also recruited in the tumor microenvironment and facilitated tumor-mediated immune escape in HNSCC.[34,35] To explore whether the anti-CD47 treatment influenced the population of MDSCs, we analyzed their populations in 2cKO mice by flow cytometry. Indeed, the percentages of CD11b$^+$ Gr-1$^+$ MDSCs were significantly decreased in CD47 treated group as compared with vehicle group. Furthermore, we found that anti-CD47 treatment decreased CD11b$^+$Ly6G$^+$Ly6C$^{lo}$ PMN-MDSCs and CD11b$^+$Ly6G$^-$ Ly6C$^{hi}$ M-MDSCs in the draining lymph nodes and rather significantly decreased PMN-MDSCs in spleen and tumor (Fig. S3C, Fig. 5D and E). This result was further confirmed by double immunofluorescence staining of CD11b$^+$ Gr1$^+$ MDSCs in aCD47 treated 2cKO mice as compared with isotype group (Fig. 5F). Quantification of immunofluorescence of CD11b$^+$Gr1$^+$MDSCs was shown in supplementary figure 3D.

### Anti-CD47 treatment regulates CD11b+ Ly6G+ MDSC function of HNSCC mouse model

To further explore the effect of anti-CD47 treatment on the immunosuppressive function of CD11b$^+$Ly6G$^+$Ly6C$^{lo}$, CD11b$^+$Ly6G$^-$Ly6C$^{hi}$, and CD4$^+$CD25$^{hi}$ Treg cells, these subsets were sorted from the spleens of anti-CD47 treated 2ckO mice and control group and cultured with CFSE-labeled effector T cells. Their capacity to suppress proliferation of effector T cells was evaluated by flow cytometry 3 days later. Results indicated that anti-CD47 treatment resulted in a decrease in suppressive function of CD11b$^+$Ly6G$^+$Ly6C$^{lo}$ MDSCs compare with the control group (Fig. S3E, Fig. 6A and B). However, when cultured with effector T cells, anti-CD47 treated CD11b$^+$Ly6G$^-$Ly6C$^{hi}$ MDSC suppressed as well as control group CD11b$^+$Ly6G$^-$Ly6C$^{hi}$ MDSC (Fig. 6C and D). And anti-CD47 treatment did not regulate the suppressive function of CD4$^+$CD25$^{hi}$ Treg cells between the groups (Fig. 6E and F).

### Anti-CD47 treatment inhibited tumor proliferation and may influence Akt-dependent pathway

The previous study reported that treatment with the TSP-1-derived peptide 4N1, a widely used CD47 agonist, facilitated the tumor proliferation via an Akt-dependent pathway.[36] Recent reports have demonstrated that PI3K/AKT/mTOR pathway was broadly activated in tumorigenesis of HNSCC.[37] To further explore the influence to proliferation through the anti-CD47 treatment, western blots of AKT, the phosphorylation status of AKT, S6 and phosphorylation status of S6 and immunohistochemistry of Ki-67 and p-AKT were performed. The anti-CD47 treatment significantly decreased

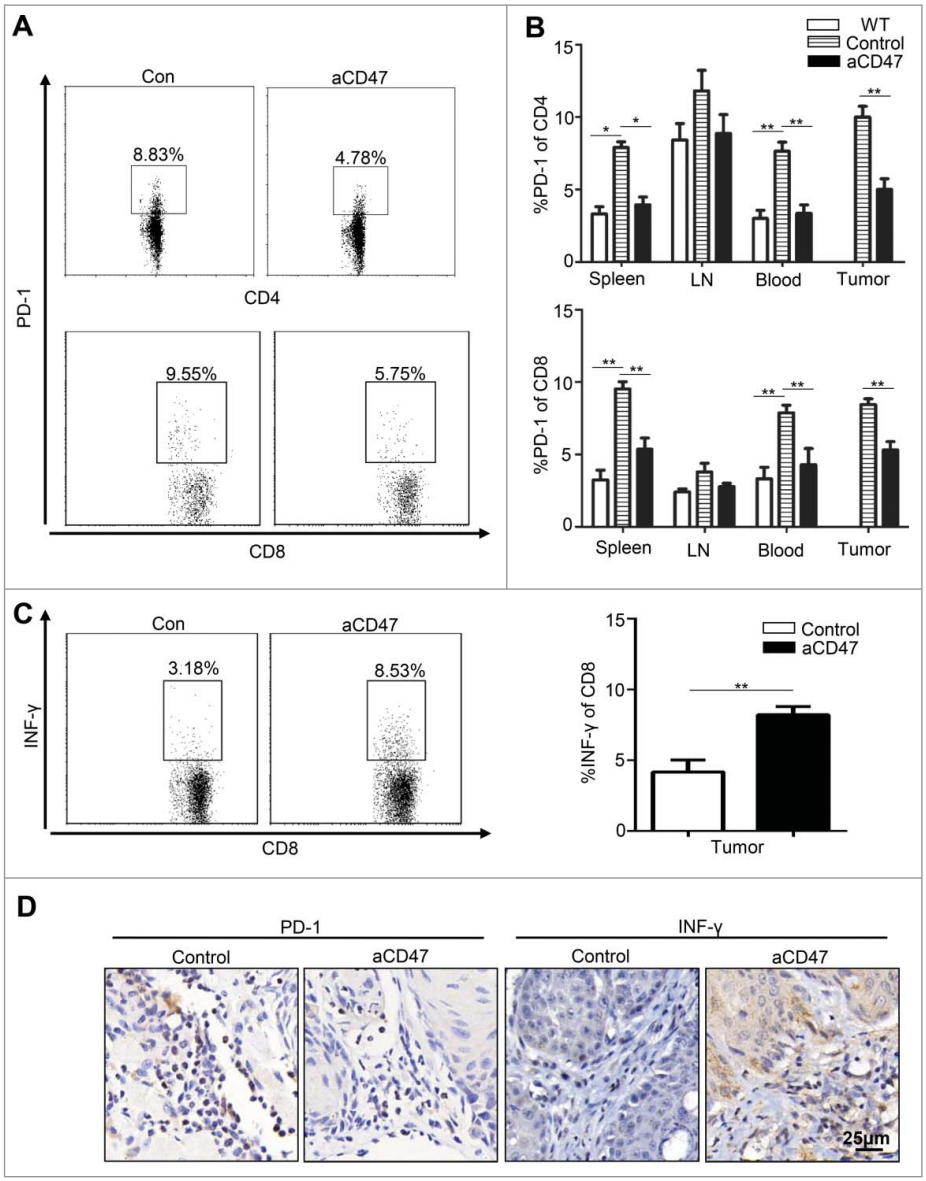


**Figure 4.** Anti-CD47 treatment improved effector T cell function in *Tgfbr1/Pten* 2 cKO mouse HNSCC model. After 4 weeks of anti-CD47 treatment (day 41), the mice were euthanized for further studies. (n = 5 mice respectively) (A) Representative flow cytometry and (B) quantification of CD47 blockade significantly decrease PD-1 expression in $CD4^+$ and $CD8^+$ T cell in aCD47 treated mouse HNSCC. (C) Representative flow cytometry and quantification of the percentage of IFN-$\gamma^+CD8^+$T cells in total $CD8^+$T cells from mice tumor (Mean ± SEM. Unpaired *t*-test,$^{**}P$-value<0.01). (D) Representative immunohistochemical staining of PD-1 and IFN-$\gamma$ in mouse HNSCC.

phospho-$S6^{S235/236}$ and phospho-$AKT^{S473}$ levels and Ki-67 level compared with isotype group (Fig. 7A and B). Meanwhile, the level of SIRP$\alpha$ was also significantly decreased in anti-CD47 treated group compared with control group (Fig. 7A). Immunofluorescence staining also confirmed the above results (Fig. 7C). Together, these results demonstrate that anti-CD47 treatment affected tumor proliferation and meanwhile, may influence Akt-dependent pathway in our HNSCC mouse model.

## Discussion

Multiple lines of evidence have shown that the immune system is a powerful tool for preventing tumor initiation as well as for eliminating tumor cells.[38,39] Immunotherapy with targeted checkpoint agents has led to remarkable advances in the treatment of cancer.[21] Emerging evidence demonstrated that dysregulation of CD47 contributed to cancer progression and tumor immune escape and the blockade of CD47 was identified as another immune checkpoint therapy.[26] We found here the expression of CD47 was significantly increased in HNSCC, which was true both in human HNSCC samples and mouse model HNSCC tissues compared with their control counterparts. Remarkably, elevated CD47 expression was correlated with positive lymph nodes and advanced HNSCC and confers poor prognosis in HNSCC patients. Interestingly, the anti-CD47 treatment could delay tumor progression and improve immunosuppressive state in immunocompetent HNSCC mouse model. Together, these results provide the rationale for using the anti-CD47 monoclonal antibody as a promising treatment for human HNSCC.

Previous study reported that anti-CD47 treatment with an anti-mouse-CD47 mAb (anti-CD47: MIAP301) could slowed the growth of tumor and reduce tumor burden in syngeneic

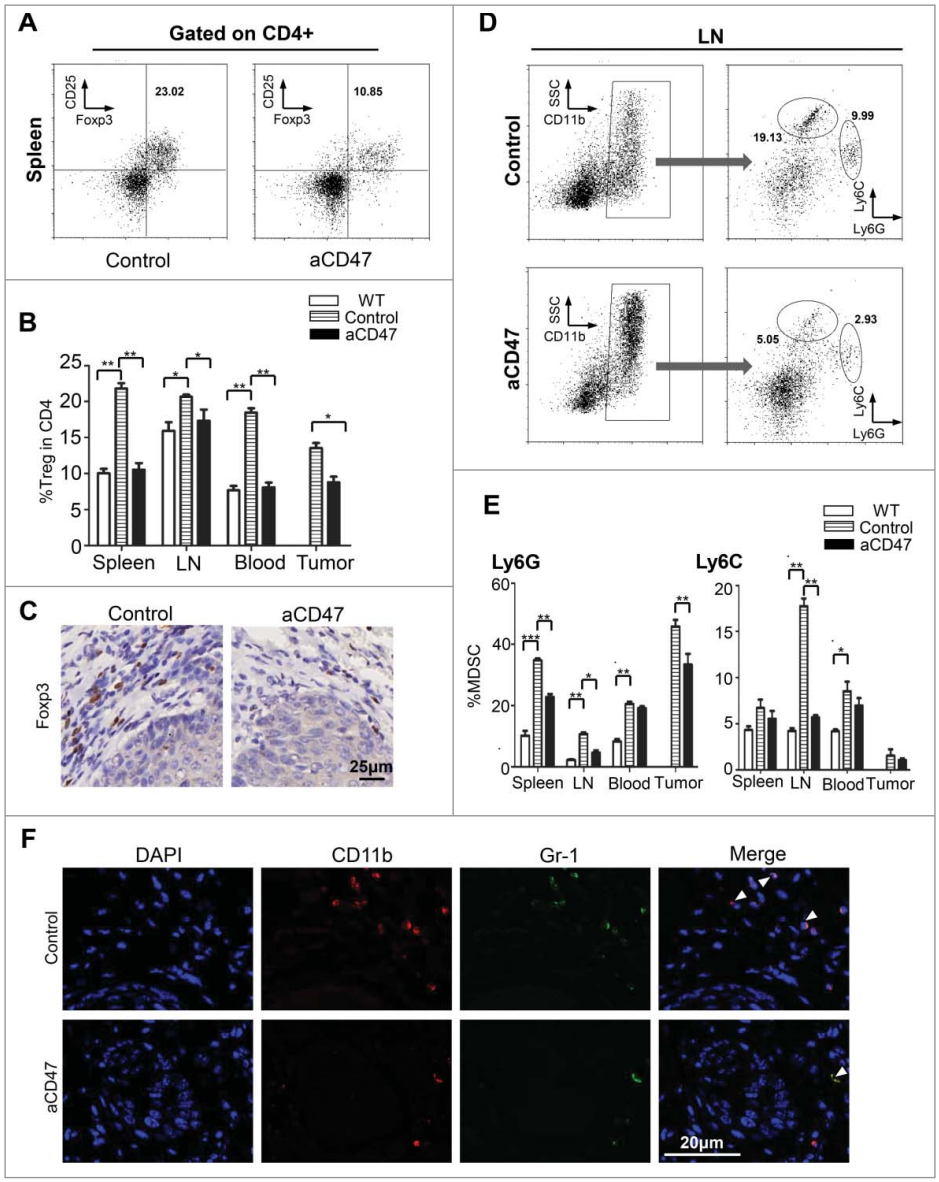


**Figure 5.** Anti-CD47 treatment significantly attenuated Tregs and MDSCs in Tgfbr1/Pten2 cKO mouse. (A) On the 41st day, the mice were euthanized for flow analysis. (n = 5 mice respectively) Representative flow cytometry plots of gating strategy of $CD4^+CD25^+$ $Foxp3^+$Tregs in the spleen. (B) Quantification of Tregs from spleen, lymph nodes (LN), peripheral blood and tumor (Mean ± SEM. Unpaired *t* test, $P < 0.05$). (C) Immunohistochemical staining of Foxp3 in aCD47 treated mouse HNSCC as compared with isotype IgG treated counterpart. (D) Representative flow cytometry plots of gating strategy of $CD11b^+Ly6G^+$ and $CD11b^+Ly6C^+$ MDSCs in lymph nodes. (E) Quantification of MDSCs (Ly6G and Ly6 C) from spleen, lymph nodes (LN), peripheral blood and tumor (Mean ± SEM. Unpaired *t*-test, $^*P < 0.05$, $^{**}P < 0.01$). (F) Representative immunofluorescence of $CD11b^+Gr1^+$MDSCs in *Tgfbr1/Pten*2 cKO mouse HNSCC in aCD47 group and isotype control group.

tumor models.[18] And another report demonstrated that anti-CD47 treatment enables phagocytosis of mouse AML.[10] Inconsistent with these reports, Willingham et al. do not show any therapeutic effects of MIAP301 in a syngeneic breast cancer model.[40] In our study, anti-CD47 treatment with MIAP301 mAb delays tumor growth in Tgfbr1/Pten 2cKO HNSCC mouse model. The reason for this difference may be due to the different tumor categories as well as the mouse model.

Previous reports described that monoclonal antibodies directed against CD47 therapy inhibited tumor progression via the enabling of phagocytosis in xenograft models.[10,41] Recent studies demonstrated inhibition of CD47 effectively enhanced antitumor the immune effect by directly triggering cytotoxic T cells in immune-competent mice.[17,18] In our study, anti-CD47 treatment effectively enhanced antitumor effects by augmenting the amount and function of effector T cells and decreasing immunosuppressive cells, regulatory T cells and MDSCs, in immunocompetent transgenic HNSCC mouse models. And anti-CD47 treatment regulates $CD11b^+$ $Ly6G^+$ MDSC function in our mouse models, which may provide an additional benefit for improving tumor immune suppressive environment. While anti-CD47 treatment does not regulate $CD11b^+$ $Ly6C^+$ MDSC. The reason for this difference is unclear and we will explore in future experiments. Van et al. reported that $CD47^{-/-}$ mice lead to selective augmentation of activated $Foxp3^+CD4^+$ Treg cells that express CD103 and CD47 expression on Treg does not regulate their function.[42] Another study reported that anti-CD47-mediated phagocytosis of cancer cells lead to a reduction in Foxp3+ regulatory T cells.[43] Our study indicated that anti-CD47 treatment decreased regulatory T cells and did not

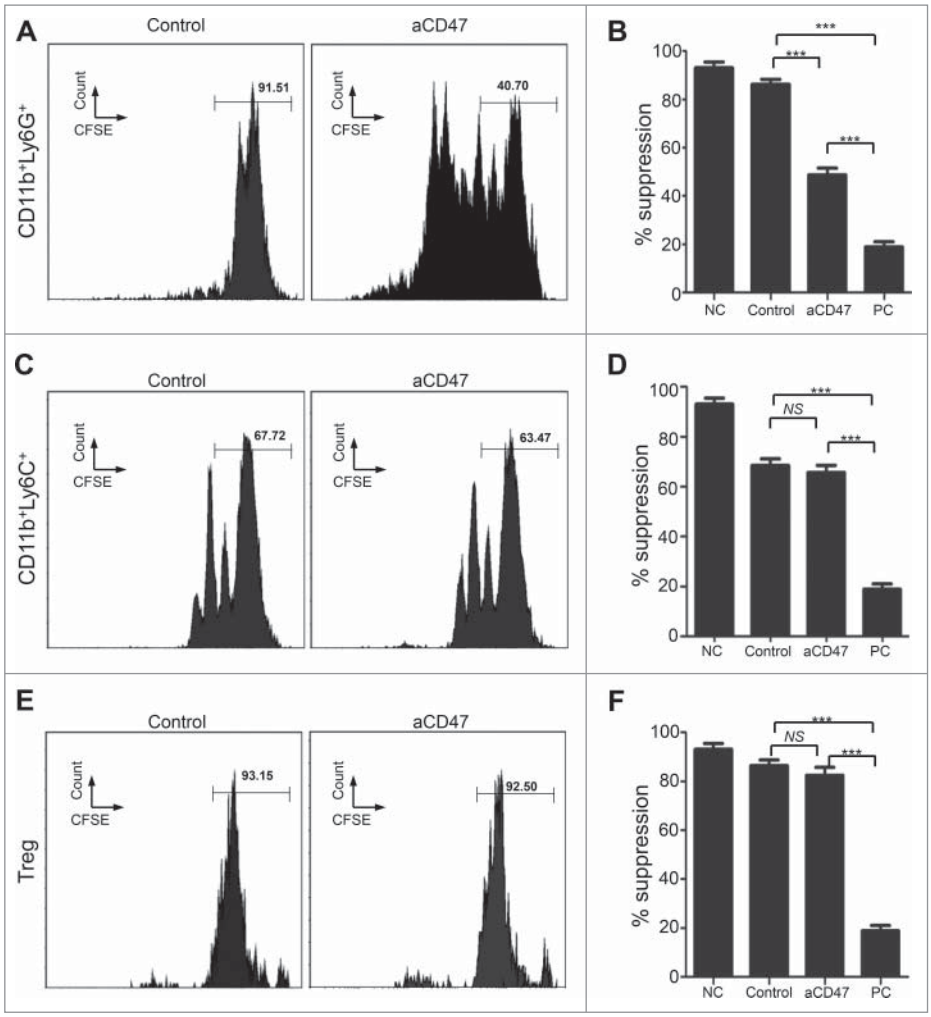


**Figure 6.** Anti-CD47 treatment regulates CD11b+ Ly6G+ MDSC function of HNSCC mouse model. (A) Representative FACS histogram of CFSE staining of activated T cells after cocultured with $CD11b^{+}Ly6G^{+}Ly6C^{lo}$ MDSCs in 72 hours. (B) Quantification of the suppressive activity of $CD11b^{+}Ly6G^{+}Ly6C^{lo}$ MDSCs between the anti-CD47 treated group and control group (NC, negative control; PC, positive control: No MDSC or Treg). (C) Representative FACS histogram of CFSE staining of activated T cells after cocultured with $CD11b^{+}Ly6G^{-}Ly6C^{hi}$ MDSCs in 72 hours. (D) Quantification of the suppressive activity of $CD11b^{+}Ly6G^{-}Ly6C^{hi}$ MDSCs between the anti-CD47 treated group and control group. (E) Representative FACS histogram of CFSE staining of activated T cells after cocultured with $CD4^{+}CD25^{hi}$ Treg cells in 72 hours. (F) Quantification of the suppressive activity of $CD4^{+}CD25^{hi}$ Treg between the anti-CD47 treated group and control group. ($^{***}P < 0.001$; *NS*: no significant).

regulate the suppressive function of $CD4^{+}CD25^{hi}$ Treg cells. Anti-CD47 cancer therapy may represent an additional approach for stimulating an effective cytotoxic T-cell response, which may contribute to antitumor effects.

Based on previous studies, these results offered the rationale for anti-CD47 alone as monotherapy for tumor therapy.[10,11] However, the combination of anti-CD47 therapy with additional therapies may induce the synergistic stimulation to eradicate tumor cells.[17,41,44,45] Chao *et al.* reveal data suggesting that the combination of anti-CD47 with anti-CD20 therapy eradicate non-Hodgkin lymphoma *in vitro* and *in vivo*.[41] Yu *et al.* reported that blockade of PD-1 down-regulated the expression of CD47 in our HNSCC mouse model,[46] which may provide a potential for the combination of anti-PD-1 and anti-CD47 treatment. Combining anti-CD47 with anti-CD40, anti-CTLA-4, anti-PD-1, or anti-PD-L1 may also lead to an increase in tumor cell elimination by the initiation of both innate and adaptive immune response. In the present study, we discovered that the anti-CD47 treatment alternate the anergic effector T cell as indicated by decrease expression PD-1 using syngeneic mouse models of cancer. Taken together, combining the therapy with anti-CD47 and alternate therapies may provide a rational candidate approach to induce tumor reduction.

The foremost important factors in cancer therapy are safety in clinical application. Immune checkpoint therapy has been reported to produce immune-driven dysimmune toxicities, defined as immune-related adverse events (irAEs), such as the anti-CTLA-4 monoclonal antibody, ipilimumab, which may be caused by unbalancing immune system.[47,48] The blockade of CD47 as another immune checkpoint therapy is also expected to take toxicity into consideration. Our results demonstrated that we did not identify readily detectable cytotoxicity in our mouse model upon anti-CD47 treatment. Although there are no reports on the toxicity of anti-CD47 treatment in the clinical study, anti-CD47 is predicted to have minimal drug toxicity due to the lack of adequate 'eat me' signals in healthy cells.[49]

In conclusion, we identified that CD47 was highly expressed in HNSCC and it is associated with clinical outcome in primary

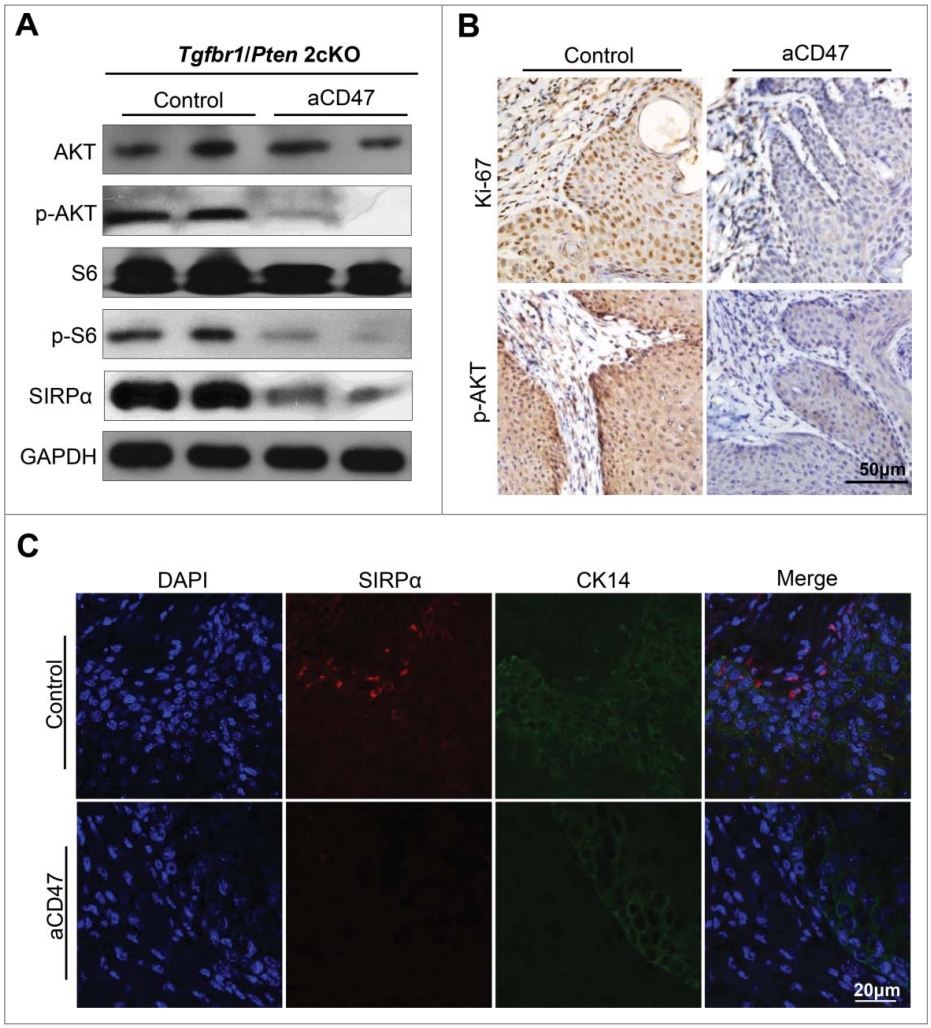


**Figure 7.** Anti-CD47 treatment influenced proliferation and may influence Akt-dependent pathway. (A) Western blot for AKT, p-AKT, S6, p-S6 and SIRP$\alpha$ in aCD47 group and isotype control group with GAPDH as a loading control. (B) Representative immunohistochemical staining of Ki-67 and p-AKT and (C) immunofluorescence staining of SIRP$\alpha$ in aCD47 group and isotype control group.

HNSCC. Blocking anti-CD47 with antibodies effectively stimulated cytotoxic T cells and improved immunosuppressive environment by decreasing immunosuppressive cells in immunocompetent HNSCC mouse model. Thus, our findings present a potential rationale for targeting CD47 for effective therapy against HNSCC in the future clinical application.

## Materials and methods

### *Immunocompetent transgenic HNSCC mouse models*

All animals and experiments were bred and performed in accordance with guidelines approved by Institutional Animal Care and Use Committee of the Wuhan University, Wuhan, China and the NIH guidelines for the use of laboratory animals in pathogen-free ASBL3 animal center of the Wuhan University. The time inducible tissue-specific *Tgfbr1/Pten* double knockout mice (*K14-Cre*$^{ERtam+/-}$; *Tgfbr1*$^{flox/flox}$; *Pten*$^{flox/flox}$, *Tgfbr1/Pten* 2cKO) were maintained and genotyped based on previous protocols.[37,50] *Tgfbr1*$^{flox/flox}$/*Pten*$^{flox/flox}$ mice (*K14-Cre*$^{ERtam+/-}$; *Tgfbr1*$^{flox/flox}$; *Pten*$^{flox/flox}$, *Tgfbr1/Pten* 2cKO) from same cage were chosen as wild type (WT) control. Tamoxifen was administered in the oral cavity of Tgfbr1/Pten 2cKO mice for 5 consecutive days to induce homozygous deletion of Tgfbr1 and Pten in head and neck epithelia.[31] All the mice had the same mixed background of FVBN/CD1/129/C57.

### *Drugs and MIAP301 treatment*

The anti-mouse CD47-blocking *in vivo* monoclonal antibody (MIAP301, rat IgG2a$\kappa$) was purchased from BioXcell (West Lebanon, NH, USA) and was stored at 4°C in the dark at a concentration of 9.87 mg/ml. The anti-CD47 antibody is a rat-derived antibody and can act by: i) CD47-SIRPa checkpoint blockade, ii) opsonisation and Fc-receptor-mediated immune effector function, or iii) both.[51] And it is known to functionally inhibit CD47-SIRP$\alpha$ interactions.[18] For the preparation of working solution, this antibody was diluted to 2 mg/ml just before use. The *in vivo* isotype control (Clone: 2A3, rat IgG2a$\kappa$) was used as an isotype control for prophylactic tumorigenesis experiments. After oral gavage with tamoxifen (2 mg/kg) for 5 consecutive days (Day 1 to Day 5), the *Tgfbr1/Pten* 2cKO mice were then treated with intraperitoneal injections of 0.2 mg of the anti-CD47 antibody or IgG control every other day from Day 12 (n = 5 mice). All animals were routinely monitored

and tumor size measurements were performed every other day. Tumor volume was calculated using the formula: tumor volume = length × width × height using a micrometer caliper.[37] The endpoint was determined based on a systematic evaluation by the veterinary doctor. Then, animals were euthanized and immune organs and tumors were harvested as soon as possible. Subsequently, the tumor tissues were fixed in formalin or frozen at −80°C for immunostaining or Western blot analysis.

### Flow cytometry

Spleen, draining lymph nodes (DLN), blood and tumors of HNSCC mouse model were processed for flow cytometric analysis as previously described.[52] Especially, the tumor tissues and immune organs were dissociated and processed by the gentleMACS Dissociator and mouse tumor dissociation kit (Miltenyi Biotec). The following anti-mouse antibodies were used for staining: FITC-conjugated anti-CD4 (Clone GK1.5), CD11b (Clone M1/70), PE-conjugated anti-Ly6G (Clone 1A8), PD1 (Clone 29F), IFN-$\gamma$ (Clone, XMG1.2) PE-Cy7-conjugated anti-Ly6C (Clone HK1.4), Percp-Cy5.5-conjugated anti-CD8 (Clone 53–6.7) and mouse regulatory T cell staining kit #3; and isotype-matched IgG controls (eBioscience, San Diego, CA). All the antibodies were used as per the manufacturer's recommended protocols. The cells were analyzed with a FACS caliber flow cytometer equipped with CellQuest software (Becton Dickinson, Mountain View, CA), and data analyzed using FlowJo (Treestar, Ashland, OR) and gated by the side scatter and forward scatter. Dead cells were excluded based on 7AAD staining (Invitrogen).

### Suppression assay

The $CD11b^{+}Ly6G^{+}Ly6C^{lo}$ MDSCs and $CD11b^{+}Ly6G^{-}Ly6C^{hi}$ MDSCs were sorted from spleens of anti-CD47 treated 2ckO mice and control group by mouse Myeloid-Derived Suppressor Cell Isolation Kit (Miltenyi Biotec, Germany). The naïve $CD8^{+}$ T cells were isolated from lymph nodes of WT mice by Naïve $CD8a^{+}$ T Cell Isolation Kit (Miltenyi Biotec, Germany). $CD4^{+}CD25^{hi}$ cells from spleens of anti-CD47 treated 2ckO mice and control group were sorted as Tregs cells by flow cytometry. The naïve CD8+ T cells were labeled with CFSE, and then were stimulated with 25 $\mu$g /ml $\alpha$CD3, 2.5 $\mu$g /ml $\alpha$CD28 and 30 IU/ml rIL-2 (BD PharmingenTM, USA). The activated T cells were respectively cocultured with $CD11b^{+}Ly6G^{+}Ly6C^{lo}$ MDSCs and $CD11b^{+}Ly6G^{-}Ly6C^{hi}$ MDSCs, and Tregs at ration of 1:1 in 96-well round-bottom plate. 72 h later, cells were assessed for CFSE analysis by flow cytometry.

### Western blot

The Western blot analysis was performed according to our previously described procedures.[53] Briefly, tumor tissues were carefully dissected and lysed with a T-PER buffer, which contains 1% phosphatase inhibitors and complete mini cocktail (Roche). Lysates of each sample were denatured and then loaded in 8–12% SDS-polyacrylamide gel electrophoresis. Subsequently, proteins were transferred to polyvinylidene fluoride membranes and blocked with milk for 1 hour, then incubated with primary antibodies: CD47 (Abcam ab175388), SIRP$\alpha$ (D6I3M), AKT (11E7), p-AKT (D9E), S6 (54D2), and p-S6 (D57.2.2E) (Cell signaling Technology) overnight. On day two, the membrane was incubated with horseradish peroxidase-conjugated secondary antibody (Pierce, Rockford, IL). The blots were developed by an enhanced chemiluminescence kit (West Pico, Thermo). GAPDH (Cell Signaling Technology) was used as a loading control. Each experiment was repeated at least three times.

### Human HNSCC samples

Human HNSCC samples were obtained from the patients in the Hospital of Stomatology of Wuhan University with informed consent. All samples were analyzed by two independent pathologists of the Department of Oral Pathology, the Wuhan University. The custom made human HNSCC tissue microarrays used in this study were described as previously.[54] The study of human tissue samples was approved by the Institutional Medical Ethics Committee of School and Hospital of Stomatology, the Wuhan University.

### Immunochemistry, images analyses, scoring system and immunofluorescence

Tumors and control counterpart tissues such as tongue mucosa were dissected from the mice and fixed in 10% formalin overnight. The tissue sections were paraffin-embedded and sectioned as previously described.[54] The sections were incubated with primary antibodies for CD47(ab175388), PD-1(D4W2J and D7D5W), PD-L1(E1L3N), Foxp3(D2W8E$^{TM}$ and D6O8R), CD11b(EPR1344), CD33 (WM53), IFN-$\gamma$ (GB11107), Ki-67 (ab15580), p-AKT (D9E) or isotype-matched IgG controls overnight. The staining was performed by ABC kits (Vector). All immunohistochemically stained slides were scanned using an Aperio ScanScope CS scanner (Vista, CA, USA). Histologic quantification of slides was operated using Aperio ScanScope quantification software (Version 9.1). The histoscore values were performed as previously described.[37,55] Briefly, histoscore of membrane and nuclear staining quantification was performed according to the formula (3+ percent cells) × 3+(2+ percent cells) × 2+(1+ percent cells) × 1 and the formula total intensity/total cell number was used to evaluate the histoscore of pixel quantification. In this case, the normalized score is 0–300. The hierarchical analysis was conducted by Cluster 3.0 with Pearson's correlation coefficient and the results were visualized by Java Treeview. Closely related biomarkers were tightly put together.[56]

For immunofluorescence staining, the slides were blocked with 10% goat serum for 1 hr and then incubated overnight at 4°C with primary antibodies:CD47(ab175388), CK14 (PROGEN German), CD11b (NB110-89474), Gr-1(RB6-8C5), SIRP$\alpha$ (D6I3M) On the second day, the sections were incubated with fluorochrome labeled secondary antibodies for 1 hr (Alexa 594 anti-rabbit Invitrogen and Alexa 488 Yeasen 34506ES60). Then, the slides were stained with 4′,6-diamidino-2-phenylindole (DAPI; Vector Laboratories). The images were detected with a laser scanning confocal microscope (Leica).

### Statistical analysis

Statistical data analysis was performed with GraphPad Prism 6.03 (GraphPad Software, Inc., La Jolla, CA) statistical packages. The data among each group were analyzed by One-way ANOVA, followed by the post-Tukey multiple comparison tests or unpaired *t* test. Two-tailed Pearson statistical analyses were used for correlated expression of these markers. Mean values ± SEM with a difference of $P < 0.05$ were considered statistically significant (ns, $p > 0.05$; $^{*}P < 0.05$; $^{**}P < 0.01$; $^{***}P < 0.001$).

## Disclosure of potential conflicts of interest

No potential conflicts of interest were disclosed.

## Financial support

This work was supported by National Natural Science Foundation of China 81472528, 81672668 (Zhi-Jun Sun), and 81472529, 81672667 (Wen-Feng Zhang). Zhi-Jun Sun was supported by the program for Fundamental Research Funds for the Central Universities (2042017kf0171).

## References

1. Hanahan D, Weinberg RA. Hallmarks of cancer: the next generation. Cell. 2011;144:646–74. doi:10.1016/j.cell.2011.02.013. PMID:21376230
2. Azoury SC, Gilmore RC, Shukla V. Molecularly targeted agents and immunotherapy for the treatment of head and neck squamous cell cancer (HNSCC). Discov Med. 2016;21:507–16. PMID:27448787.
3. Murdoch C, Muthana M, Coffelt SB, Lewis CE. The role of myeloid cells in the promotion of tumour angiogenesis. Nat Rev Cancer. 2008;8:618–31. doi:10.1038/nrc2444. PMID:18633355.
4. Gabrilovich DI, Nagaraj S. Myeloid-derived suppressor cells as regulators of the immune system. Nat Rev Immunol. 2009;9:162–74. doi:10.1038/nri2506. PMID:19197294.
5. Peng D, Tanikawa T, Li W, Zhao L, Vatan L, Szeliga W, Wan S, Wei S, Wang Y, Liu Y, et al. Myeloid-Derived Suppressor Cells Endow Stem-like Qualities to Breast Cancer Cells through IL6/STAT3 and NO/NOTCH Cross-talk Signaling. Cancer Res. 2016;76:3156–65. doi:10.1158/0008-5472.CAN-15-2528. PMID:27197152.
6. Nagaraj S, Gupta K, Pisarev V, Kinarsky L, Sherman S, Kang L, Herber DL, Schneck J, Gabrilovich DI. Altered recognition of antigen is a mechanism of CD8+ T cell tolerance in cancer. Nat Med. 2007;13:828–35. doi:10.1038/nm1609. PMID:17603493.
7. Bronte V, Brandau S, Chen SH, Colombo MP, Frey AB, Greten TF, Mandruzzato S, Murray PJ, Ochoa A, Ostrand-Rosenberg S, et al. Recommendations for myeloid-derived suppressor cell nomenclature and characterization standards. Nat Commun. 2016;7:12150. doi:10.1038/ncomms12150. PMID:27381735.
8. Li MO, Rudensky AY. T cell receptor signalling in the control of regulatory T cell differentiation and function. Nat Rev Immunol. 2016;16:220–33. doi:10.1038/nri.2016.26. PMID:27026074.
9. Nishiyama Y, Tanaka T, Naitoh H, Mori C, Fukumoto M, Hiai H, Toyokuni S. Overexpression of integrin-associated protein (CD47) in rat kidney treated with a renal carcinogen, ferric nitrilotriacetate. Jpn J Cancer Res. 1997;88:120–8. doi:10.1111/j.1349-7006.1997.tb00356.x. PMID:9119739.
10. Majeti R, Chao MP, Alizadeh AA, Pang WW, Jaiswal S, Gibbs KD, Jr., van Rooijen N, Weissman IL. CD47 is an adverse prognostic factor and therapeutic antibody target on human acute myeloid leukemia stem cells. Cell. 2009;138:286–99. doi:10.1016/j.cell.2009.05.045. PMID:19632179.
11. Xiao Z, Chung H, Banan B, Manning PT, Ott KC, Lin S, Capoccia BJ, Subramanian V, Hiebsch RR, Upadhya GA, et al. Antibody mediated therapy targeting CD47 inhibits tumor progression of hepatocellular carcinoma. Cancer Lett. 2015;360:302–9. doi:10.1016/j.canlet.2015.02.036. PMID:25721088.
12. Campbell IG, Freemont PS, Foulkes W, Trowsdale J. An ovarian tumor marker with homology to vaccinia virus contains an IgV-like region and multiple transmembrane domains. Cancer Res. 1992;52:5416–20. PMID:1394148.
13. Chao MP, Weissman IL, Majeti R. The CD47-SIRPalpha pathway in cancer immune evasion and potential therapeutic implications. Curr Opin Immunol. 2012;24:225–32. doi:10.1016/j.coi.2012.01.010. PMID:22310103.
14. Brooke G, Holbrook JD, Brown MH, Barclay AN. Human lymphocytes interact directly with CD47 through a novel member of the signal regulatory protein (SIRP) family. J Immunol. 2004;173:2562–70. doi:10.4049/jimmunol.173.4.2562. PMID:15294972.
15. Li Z, He L, Wilson K, Roberts D. Thrombospondin-1 inhibits TCR-mediated T lymphocyte early activation. J Immunol. 2001;166:2427–36. doi:10.4049/jimmunol.166.4.2427. PMID:11160302.
16. Kaur S, Kuznetsova SA, Pendrak ML, Sipes JM, Romeo MJ, Li Z, Zhang L, Roberts DD. Heparan sulfate modification of the transmembrane receptor CD47 is necessary for inhibition of T cell receptor signaling by thrombospondin-1. J Biol Chem. 2011;286:14991–5002. doi:10.1074/jbc.M110.179663. PMID:21343308.
17. Soto-Pantoja DR, Terabe M, Ghosh A, Ridnour LA, DeGraff WG, Wink DA, Berzofsky JA, Roberts DD. CD47 in the tumor microenvironment limits cooperation between antitumor T-cell immunity and radiotherapy. Cancer Res. 2014;74:6771–83. doi:10.1158/0008-5472.CAN-14-0037-T. PMID:25297630.
18. Liu X, Pu Y, Cron K, Deng L, Kline J, Frazier WA, Xu H, Peng H, Fu YX, Xu MM. CD47 blockade triggers T cell-mediated destruction of immunogenic tumors. Nat Med. 2015;21:1209–15. doi:10.1038/nm.3931. PMID:26322579.
19. Chan KS, Espinosa I, Chao M, Wong D, Ailles L, Diehn M, Gill H, Presti J, Jr., Chang HY, van de Rijn M, et al. Identification, molecular characterization, clinical prognosis, and therapeutic targeting of human bladder tumor-initiating cells. Proc Natl Acad Sci U S A. 2009;106:14016–21. doi:10.1073/pnas.0906549106. PMID:19666525.
20. Manna PP, Frazier WA. CD47 mediates killing of breast tumor cells via Gi-dependent inhibition of protein kinase A. Cancer Res. 2004;64:1026–36. doi:10.1158/0008-5472.CAN-03-1708. PMID:14871834.
21. Pardoll DM. The blockade of immune checkpoints in cancer immunotherapy. Nat Rev Cancer. 2012;12:252–64. doi:10.1038/nrc3239. PMID:22437870
22. Kim MJ, Lee JC, Lee JJ, Kim S, Lee SG, Park SW, Sung MW, Heo DS. Association of CD47 with natural killer cell-mediated cytotoxicity of head-and-neck squamous cell carcinoma lines. Tumour Biol. 2008;29:28–34. PMID:18497546. doi:10.1159/000132568.
23. Maxhimer JB, Soto-Pantoja DR, Ridnour LA, Shih HB, Degraff WG, Tsokos M, Wink DA, Isenberg JS, Roberts DD. Radioprotection in normal tissue and delayed tumor growth by blockade of CD47 signaling. Sci Transl Med. 2009;1:3ra7. doi:10.1126/scitranslmed.3000139. PMID:20161613
24. Yang C, Gao S, Zhang H, Xu L, Liu J, Wang M, Zhang S. CD47 is a Potential Target for the Treatment of Laryngeal Squamous Cell Carcinoma. Cell Physiol Biochem. 2016;40:126–36. doi:10.1159/000452530. PMID:27855370.
25. Rhodes DR, Kalyana-Sundaram S, Mahavisno V, Varambally R, Yu J, Briggs BB, Barrette TR, Anstet MJ, Kincead-Beal C, Kulkarni P, et al. Oncomine 3.0: genes, pathways, and networks in a collection of 18,000 cancer gene expression profiles. Neoplasia. 2007;9:166–80. doi:10.1593/neo.07112. PMID:17356713.
26. Vonderheide RH. CD47 blockade as another immune checkpoint therapy for cancer. Nat Med. 2015;21:1122–3. doi:10.1038/nm.3965. PMID:26444633.
27. Ferris RL. Immunology and Immunotherapy of Head and Neck Cancer. J Clin Oncol. 2015;33:3293–304. doi:10.1200/JCO.2015.61.1509. PMID:26351330
28. Leemans CR, Braakhuis BJ, Brakenhoff RH. The molecular biology of head and neck cancer. Nat Rev Cancer. 2011;11:9–22. https://dx.doi.org/10.1038/nrc2982. PMID:21160525.

29. Honjo Y, Bian Y, Kawakami K, Molinolo A, Longenecker G, Boppana R, Larsson J, Karlsson S, Gutkind JS, Puri RK, et al. TGF-beta receptor I conditional knockout mice develop spontaneous squamous cell carcinoma. Cell Cycle. 2007;6:1360–6. doi:10.4161/cc.6.11.4268. PMID:17534148.
30. Bian Y, Terse A, Du J, Hall B, Molinolo A, Zhang P, Chen W, Flanders KC, Gutkind JS, Wakefield LM, et al. Progressive tumor formation in mice with conditional deletion of TGF-beta signaling in head and neck epithelia is associated with activation of the PI3K/Akt pathway. Cancer Res. 2009;69:5918–26. doi:10.1158/0008-5472.CAN-08-4623. PMID:19584284.
31. Bian Y, Hall B, Sun ZJ, Molinolo A, Chen W, Gutkind JS, Waes CV, Kulkarni AB. Loss of TGF-beta signaling and PTEN promotes head and neck squamous cell carcinoma through cellular senescence evasion and cancer-related inflammation. Oncogene. 2012;31:3322–32. doi:10.1038/onc.2011.494. PMID:22037217.
32. Wherry EJ. T cell exhaustion. Nat Immunol. 2011;12:492–9. PMID:21739672.
33. Yu GT, Bu LL, Zhao YY, Mao L, Deng WW, Wu TF, Zhang WF, Sun ZJ. CTLA4 blockade reduces immature myeloid cells in head and neck squamous cell carcinoma. Oncoimmunology. 2016;5:e1151594. doi:10.1080/2162402X.2016.1151594. PMID:27471622.
34. Freiser ME, Serafini P, Weed DT. The immune system and head and neck squamous cell carcinoma: from carcinogenesis to new therapeutic opportunities. Immunol Res. 2013;57:52–69. doi:10.1007/s12026-013-8462-3. PMID:24218361.
35. Stagg J, Smyth MJ. Extracellular adenosine triphosphate and adenosine in cancer. Oncogene. 2010;29:5346–58. doi:10.1038/onc.2010.292. PMID:20661219.
36. Sick E, Boukhari A, Deramaudt T, Ronde P, Bucher B, Andre P, Gies JP, Takeda K. Activation of CD47 receptors causes proliferation of human astrocytoma but not normal astrocytes via an Akt-dependent pathway. Glia. 2011;59:308–19. doi:10.1002/glia.21102. PMID:21125662.
37. Sun ZJ, Zhang L, Hall B, Bian Y, Gutkind JS, Kulkarni AB. Chemopreventive and chemotherapeutic actions of mTOR inhibitor in genetically defined head and neck squamous cell carcinoma mouse model. Clin Cancer Res. 2012;18:5304–13. doi:10.1158/1078-0432.CCR-12-1371. PMID:22859719.
38. Palucka AK, Coussens LM. The Basis of Oncoimmunology. Cell. 2016;164:1233–47. doi:10.1016/j.cell.2016.01.049. PMID:26967289.
39. Raval RR, Sharabi AB, Walker AJ, Drake CG, Sharma P. Tumor immunology and cancer immunotherapy: summary of the 2013 SITC primer. J Immunother Cancer. 2014;2:14. doi:10.1186/2051-1426-2-14. PMID:24883190
40. Willingham SB, Volkmer JP, Gentles AJ, Sahoo D, Dalerba P, Mitra SS, Wang J, Contreras-Trujillo H, Martin R, Cohen JD, et al. The CD47-signal regulatory protein alpha (SIRPa) interaction is a therapeutic target for human solid tumors. Proc Natl Acad Sci U S A. 2012;109:6662–7. doi:10.1073/pnas.1121623109. PMID:22451913.
41. Chao MP, Alizadeh AA, Tang C, Myklebust JH, Varghese B, Gill S, Jan M, Cha AC, Chan CK, Tan BT, et al. Anti-CD47 antibody synergizes with rituximab to promote phagocytosis and eradicate non-Hodgkin lymphoma. Cell. 2010;142:699–713. doi:10.1016/j.cell.2010.07.044. PMID:20813259.
42. Van VQ, Darwiche J, Raymond M, Lesage S, Bouguermouh S, Rubio M, Sarfati M. Cutting edge: CD47 controls the in vivo proliferation and homeostasis of peripheral CD4+ CD25+ Foxp3+ regulatory T cells that express CD103. J Immunol. 2008;181:5204–8. doi:10.4049/jimmunol.181.8.5204. PMID:18832672.
43. Tseng D, Volkmer JP, Willingham SB, Contreras-Trujillo H, Fathman JW, Fernhoff NB, Seita J, Inlay MA, Weiskopf K, Miyanishi M, et al. Anti-CD47 antibody-mediated phagocytosis of cancer by macrophages primes an effective antitumor T-cell response. Proc Natl Acad Sci U S A. 2013;110:11103–8. doi:10.1073/pnas.1305569110. PMID:23690610
44. Lo J, Lau EY, So FT, Lu P, Chan VS, Cheung VC, Ching RH, Cheng BY, Ma MK, Ng IO, et al. Anti-CD47 antibody suppresses tumour growth and augments the effect of chemotherapy treatment in hepatocellular carcinoma. Liver Int. 2016;36:737–45. doi:10.1111/liv.12963. PMID:26351778.
45. Ngo M, Han A, Lakatos A, Sahoo D, Hachey SJ, Weiskopf K, Beck AH, Weissman IL, Boiko AD. Antibody Therapy Targeting CD47 and CD271 Effectively Suppresses Melanoma Metastasis in Patient-Derived Xenografts. Cell Rep. 2016;16:1701–16. doi:10.1016/j.celrep.2016.07.004. PMID:27477289.
46. Yu GT, Bu LL, Huang CF, Zhang WF, Chen WJ, Gutkind JS, Kulkarni AB, Sun ZJ. PD-1 blockade attenuates immunosuppressive myeloid cells due to inhibition of CD47/SIRPalpha axis in HPV negative head and neck squamous cell carcinoma. Oncotarget. 2015;6:42067–80. doi:10.18632/oncotarget.5955. PMID:26573233.
47. Gao J, He Q, Subudhi S, Aparicio A, Zurita-Saavedra A, Lee DH, Jimenez C, Suarez-Almazor M, Sharma P. Review of immune-related adverse events in prostate cancer patients treated with ipilimumab: MD Anderson experience. Oncogene. 2015;34:5411–7. doi:10.1038/onc.2015.5. PMID:25659583.
48. Boutros C, Tarhini A, Routier E, Lambotte O, Ladurie FL, Carbonnel F, Izzeddine H, Marabelle A, Champiat S, Berdelou A, et al. Safety profiles of anti-CTLA-4 and anti-PD-1 antibodies alone and in combination. Nat Rev Clin Oncol. 2016;13:473–86. doi:10.1038/nrclinonc.2016.58. PMID:27141885.
49. McCracken MN, Cha AC, Weissman IL. Molecular Pathways: Activating T Cells after Cancer Cell Phagocytosis from Blockade of CD47 "Don't Eat Me" Signals. Clin Cancer Res. 2015;21:3597–601. doi:10.1158/1078-0432.CCR-14-2520. PMID:26116271.
50. Zhang L, Sun ZJ, Bian Y, Kulkarni AB. MicroRNA-135b acts as a tumor promoter by targeting the hypoxia-inducible factor pathway in genetically defined mouse model of head and neck squamous cell carcinoma. Cancer Lett. 2013;331:230–8. doi:10.1016/j.canlet.2013.01.003. PMID:23340180.
51. Oldenborg PA, Gresham HD, Lindberg FP. CD47-signal regulatory protein alpha (SIRPalpha) regulates Fcgamma and complement receptor-mediated phagocytosis. J Exp Med. 2001;193:855–62. doi:10.1084/jem.193.7.855. PMID:11283158.
52. Deng WW, Mao L, Yu GT, Bu LL, Ma SR, Liu B, Gutkind JS, Kulkarni AB, Zhang WF, Sun ZJ. LAG-3 confers poor prognosis and its blockade reshapes antitumor response in head and neck squamous cell carcinoma. Oncoimmunology. 2016;5:e1239005. doi:10.1080/2162402X.2016.1239005. PMID:27999760
53. Woodman N, Pinder SE, Tajadura V, Le BX, Gillett C, Delannoy P, Burchell JM, Julien S. Two E-selectin ligands, BST-2 and LGALS3BP, predict metastasis and poor survival of ER-negative breast cancer. Int J Oncol. 2016;49:265. PMID:27176937
54. Wu L, Deng WW, Yu GT, Mao L, Bu LL, Ma SR, Liu B, Zhang WF, Sun ZJ. B7-H4 expression indicates poor prognosis of oral squamous cell carcinoma. Cancer Immunol Immunother. 2016;65:1035–45. doi:10.1007/s00262-016-1867-9. PMID:27383830.
55. Wu L, Deng WW, Huang CF, Bu LL, Yu GT, Mao L, Zhang WF, Liu B, Sun ZJ. Expression of VISTA correlated with immunosuppression and synergized with CD8 to predict survival in human oral squamous cell carcinoma. Cancer Immunol Immunother. 2017;66:627–36. doi:10.1007/s00262-017-1968-0. PMID:28236118.
56. Eisen MB, Spellman PT, Brown PO, Botstein D. Cluster analysis and display of genome-wide expression patterns. Proc Natl Acad Sci U S A. 1998;95:14863–8. doi:10.1073/pnas.95.25.14863. PMID:9843981.